Defence Science Journal, Vol. 75, No. 3, May 2025, pp. 379-385, DOI : 10.14429/dsj.20789

Measurement of Shake in the Camera in a Shelling Zone

Manoj Sharma[#,*], Subrat Kar[$] and Sumantra Dutta Roy[$]

[#]DRDO-Directorate of Information Technology and Cyber Security, New Delhi - 110 011, India
[$]Department of Electrical Engineering, IIT Delhi, Delhi - 110 016, India
[*]E-mail: manoj.hqr@gov.in

ABSTRACT

The stability of the camera in an imaging system stationed for the measurement of coordinates of moving objects is of paramount importance, failing which system can generate erroneous results leading to loss of higher order1. Losses can be as high as human lives in a battlefield scenario where tracking the moving object and measuring its coordinates in real-time is crucial for countermeasures against such moving objects/ threats. This paper presents a technique that uses the basic properties of an imaging system and existing corner detection techniques to measure the movement caused in the camera due to shaking of the ground. A system with a camera pair is discussed in this paper as a case for understanding the effects of shaking of the ground on the imaging system. A solution is devised to measure these effects and feed them to a feasible compensation system. It can always lead to realizing a system with minimum errors to maximize the saving of human lives.

Keywords: Ground shake; Artillery; Projectile; Tracking; Stereoscopic imaging; Angular measurement; Corner detection; Shake-compensation

1. INTRODUCTION

In modern artillery, the firing takes place from a distance up to 30 km to 50 km away from the point of impact[2]. The trajectory of the shell may be visible (in the air) for 2 sec. to 5 sec. and the trajectory or flight path while the shell is in the air is the only basis, we have to determine the possible point of origin given the geo-information of the area. In one of the previous works, expressions have been derived for the measurement of relative 3D coordinates given by X_n, Y_n and Z_n. These values are the distances of the detected shell from the camera along three global coordinate axes. Subscript n in by X_n, Y_n and Z_n represents the nth frame and hence values of relative coordinates for all frames have to be captured in real time using mathematical expressions. It is evident in mathematical expressions[3] that depth is calculated first, leading to values for all three relative coordinates. These dependencies are explained as (i) Z (Depth), which depends upon b (baseline), p(pixel size of the camera), and f (focal length of the camera) (ii) Z_n (Distance of the target along Z axis) which depends upon Z, θ_x and θ_y where the latter are the angles that the orientation of the camera makes with the global coordinates X and Y (iii) X_n (Distance of the target along X axis) which depends upon Z_n, and θ_x and (iv) Y_n (Distance of the target along Y axis) which depends upon Z_n, and θ_y.

In the physical zone of firing, shells are fired from the adversary side near the camera set up and shells can keep on exploding in the nearby region in a time gap of few seconds. Due to frequent shelling, sudden shocks are generated near the setup that makes the ground shake[4-5]. Looking at the dependencies of the parameters on the final value of calculations of relative coordinates, baseline, pixel size, and focal length are invariant of the ground shake and do not cause any change in desired calculations due to ground shake during the explosion of shells.

Received : 23 October 2024, Revised : 05 December 2024
Accepted : 11 April 2025, Online published : 08 May 2025

2. EFFECT OF GROUND SHAKE ON THE PARAMETERS

In this section, we will discuss how Ground Shake affects these parameters and thus affect calculations being done for the estimation of the location of the target. Since these calculations are targeted at a higher rate as we intend to capture the shell at a frame rate of 24 fps, the accuracy of the results becomes a vital factor. Prominent movement due to seismic vibrations caused by shell explosions is a rhythmic movement in the physical world. Seismic vibrations have been studied in detail by researchers for their motion characteristics[6-8]. If cameras are tied on two cantilevers with the center at Point C and also have one joint each at two cantilevers at Point A and B respectively. The whole assembly might experience a movement as shown in Fig. 1.

Assembly holding Cameras C_R and C_L is centered at C and is holding both cameras 10 m apart in a vertically aligned position. As discussed earlier, if both cameras are held using cantilevers CC_L and CC_R, these are bound to have rhythmic sway movements due to the shaking of the ground. These movements can occur in both X and Y directions for the cameras. As shown in Fig. 1, the spin of the camera is not possible as cameras are tightly bound to the assembly. On the left section of the image, all possible rhythmic movements of the cameras are shown. C_LCC_R the line shown in bold is the normal alignment

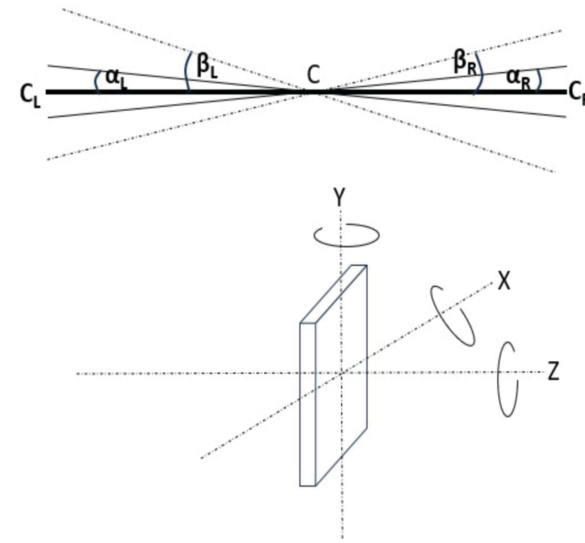

Figure 1: Angular movement.

of the cameras, and both are aligned. Shaking in the ground can cause the cameras to move in the same and opposite directions, both horizontally and vertically. Solid lines shown in the light shade depict movements along the X coordinate, and any movement can make a rotation of the left camera with an angle α_L with the original position. Similarly right camera can have a rotation with an angle α_R due to sway movements. Both cameras will also have some component of movement along the Y coordinate, which causes the rotation of the cameras with an angle β_L and β_R respectively for left and right cameras, and these movements are shown as dotted lines deviating from CC_L and CC_R.

As discussed earlier, camera assembly has a rotation of θ_x and θ_y regarding the global X and Y coordinates. If the movement of the camera assembly is in the same direction of rotation, $\cos\theta_x$ should be replaced with $\cos(\theta_x + \alpha_L)$ in the calculations of relative coordinates in the previous chapter. Similarly, if the movement of the assembly is in the opposite direction, $\cos\theta_x$ should be replaced by $\cos(\theta_x - \alpha_L)$ in the calculations. Videos were generated using the Blender tool to calculate the world point coordinates of the target at the point of capturing and hence the trajectory of motion of the shell after it is fired. Table 1 given below shows the effect of shakes in pan and tilt movement on individual cameras on the measurement of the difference between the position of the target in the left and right camera.

Points that can be concluded from the table above are the following: -

- If both cameras are moving with the same degree of rotation in all directions, there is no change in values of disparity and hence in the results. There will be a change in window size for the tracking of the shell.
- If both cameras have tilted only, even with different magnitudes, there is no change in disparity.
- If both cameras have different values of pan movement due to shaking of the ground or any other reason, the proposed method of calculation will fail as it assumes that the planes of sensors of both cameras are perfectly aligned[9].

3. SHAKE COMPENSATION BEFORE MEASUREMENT

Movement due to explosions can lead to oscillations that eventually make the camera come to rest after some time. These oscillations are followed by both the cameras together but the transition in position and angles of both cameras can be different making it a problem to be addressed[10,11]. We consider the case of a single camera first and then consider a similar case for a stereoscopic pair to find out its effect and remedy but measurement or the estimation of the motion is an essential requirement[12-14]. Suppose a point, henceforth called a reference point in the image, is present at (R_x, R_y) in the image plane and it is not expected to change in normal circumstances. This usually can be a fixed point nearby or a point on the mountain depending upon the ambience of deployment. Figure 2 shows the movement this point can have in the image following the ground shake due to the explosion.

Once the displacement of the reference point in the image plane is found, it can lead to correction of the position of the camera-pair and thus compensate for the effect of ground shake. There are the following existing ways to compensate for the shaking effects in the cameras: -

- Gyro sensors-based Electronic controlled platforms are commercially available to cater for shake compensations[15-17]. In the context of our problem,

Table 1. Effect on disparity due to shaking of ground

Frame No	Difference in pixels without shake	For $+1^0$ tilt in left cam	Difference in pixels for $+2^0$ tilt in right cam	Difference in pixels for $+1^0$ pan in left cam	Difference in pixels for $+1^0$ pan in right cam	Difference in pixels for $+1^0$ pan in both cams
291	97	97	97	322	-128	97
292	97.5	97.5	97.5	322.5	-127.5	97.5
293	98	98	98	323	-127	98
294	98.5	98.5	98.5	323.5	-126.5	98.5
295	99	99	99	324	-126	99
296	100	100	100	325	-125	100
297	100.5	100.5	100.5	325.5	-124.5	100.5
298	101	101	101	326	-124	101
299	102	102	102	327	-123	102
300	102	102	102	327	-123	102

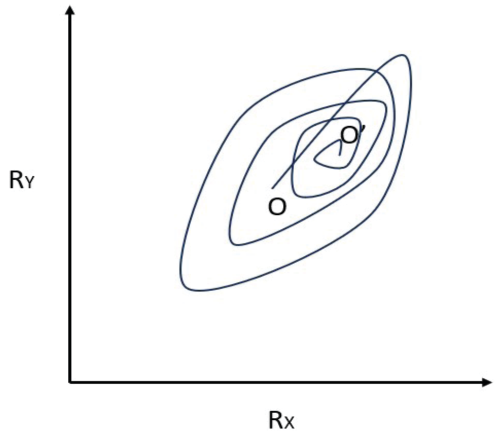

Figure 2. Movement of reference point in the image.

stereoscopic assembly has to be a payload to such an actuation system which will try to minimize the effects of ground shake on the results of relative coordinates.

- Many Image Processing techniques are available for image stabilization in case of shake in an imaging device[18-21]. Similar work has been carried out to understand shake's effects on the stereoscopic setup of multiple cameras.

3.1 Estimation of Effects Due to Ground-Shake

Before compensation is affected for the movement of cameras individually, it is required to measure the changes in camera orientation due to shaking of the ground. In the stable state of the camera pair when there is no shaking of the cameras, we can identify certain points in the image of each camera that are expected to be stable during the use of this system. It can be a point on a hill, a rock, or any other near or distant point on a stable object. We can find out its coordinates in the image before and after the shake to ascertain the degree to which the camera has drifted/ tilted. It is explained in detail in Fig. 3.

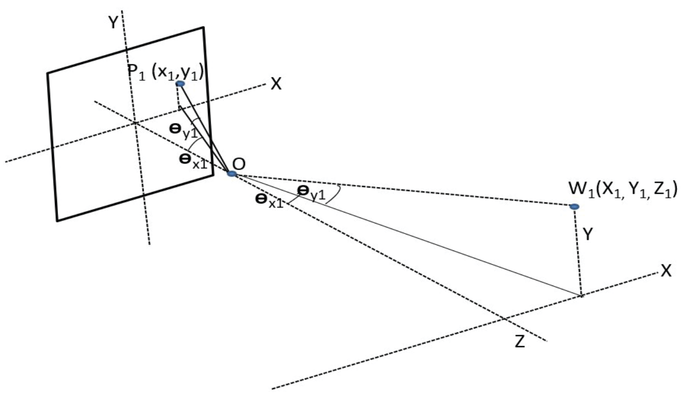

Figure 3. Estimating angular movement of camera.

Suppose there is a point W_1 in the field of view of a camera having an optical center O and an image sensor shown in the rectangle in Fig. 3. The point has world coordinates (X_1, Y_1, Z_1) and is projected at the pixel P_1 on the image sensor. Suppose the coordinates of the sensor's center are (x_C, y_C) and pixel P_1 has coordinates (X_1, Y_1). There are two pairs of similar triangles with θ_{x1} and θ_{y1} as equal angles in different pairs. The following two Eqn., Eqn. 1 and Eqn. 2 give values for these angles: -

$$\theta_{x1} = \tan^{-1} \frac{p(x_1 - x_c)}{f} \tag{1}$$

$$\theta_{y1} = \tan^{-1} \frac{p(y_1 - y_c)}{f} \tag{2}$$

p is the pixel size of the image sensor and is uniform in both axes, i.e., every pixel is a perfect square. f is the focal length of the camera and it is equal to the distance between the optical center of the camera and the center of the sensor. It is required to devise a method to find out the location of the same point in the image as it is assumed to be moved due to the movement of the camera. Suppose it is projected at the pixel P_2 with coordinates (x_2, y_2). This point forms angles θ_{x2} and θ_{y2} along the X and Y axes from the optical axis of the sensor and these angles are given by the following equations, Eqn. 3 and Eqn. 4: -

$$\theta_{x2} = \tan^{-1} \frac{p(x_2 - x_c)}{f} \tag{3}$$

$$\theta_{y2} = \tan^{-1} \frac{p(y_2 - y_c)}{f} \tag{4}$$

These equations are based on assumptions that the optics of both the cameras are uniform and linear in characteristics and placement of the sensor is exactly at the focal length from the lens. Further, angular disturbances created due to the shaking of the ground are measured by changes in these angles. If we can calculate $\theta_{x2} - \theta_{x1}$ and $\theta_{y2} - \theta_{y1}$, we can correct the angular position of the cameras to make it a stereoscopic pair as described in an ideal case.

3.2 RESULTS

Two procedures were followed to have results and verification of the concept discussed in the section: Manual and based on Image Processing. In the scenario of deployment of the proposed system, if the reference images of the scene for both cameras are taken independently before use and a reference point is marked with its coordinates, it can be used to measure the change of orientation of the cameras later on. For instance, manually marking a point in the image beforehand and finding its coordinates using any simple code was carried out. Later, after inducing some angular change in both axes in the orientation of the camera simulated the effects of shaking the ground. This resulted in a tilted image and thus finding out the coordinates of the same marked point in the image can lead to the information required to implement the method discussed in this section to calculate the change in the orientation of the camera using the Eqn. 1, 2, 3 & 4. Table 2 shows the values of the angular change measured using formulae:

Table 2. Induced vs measured changes

Axes	Induced change (Deg)	Measured change (Deg)
X	1	0.989
X	2	1.88
Y	1	0.996
Y	2	2.07

Although this technique gives results that are close to the expected one, it has a limitation also. This technique requires manual intervention, and since the point must be marked manually, there is a high chance of error in marking the same pixel as the center. To avoid errors in manual methods, certain proven techniques can be utilized for the automated matching of points or features in a pair of images that have a shift in the scene due to shaking or other movements. The following are the ones being widely used:

- Harris Corner Detection[22]
- Shi-Tomasi Corner Detector[23]
- Scale Invariant Feature Transform (SIFT)[24]
- Speeded Up Robust Features (SURF)[25]
- Features from Accelerated Segment Test (FAST) algorithm for corner detection[26]

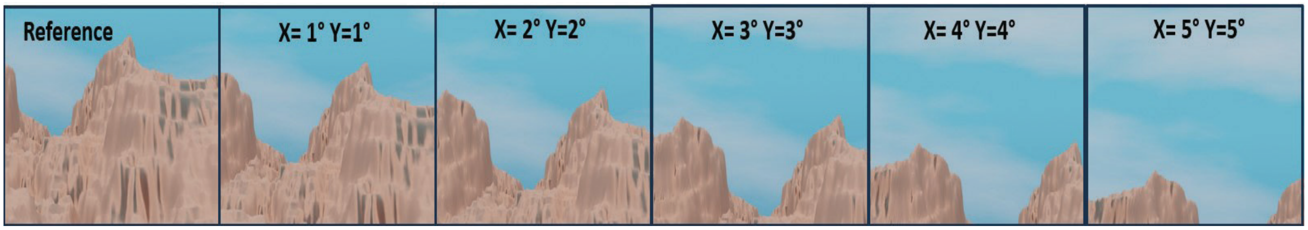

Figure 4. Reference scene and shifts of 1° to 5° in both directions.

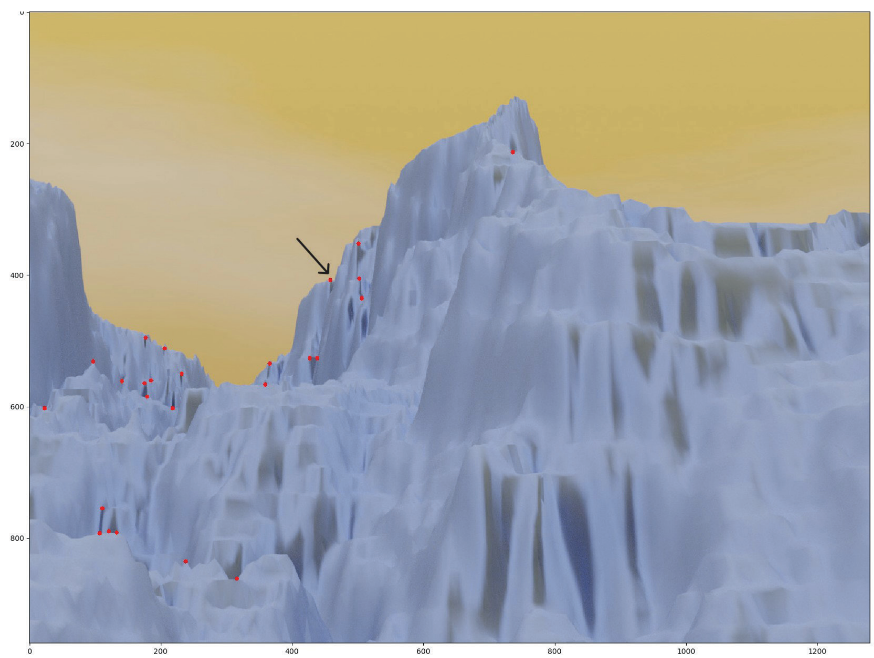

Figure 5: Reference scene with red dots as marked points' locations.

Figure 6. Shift of 1° in both axes in the scene with red dots as marked points' locations.

- Binary Robust Independent Elementary Features (BRIEF)[27]
- Oriented FAST and Rotated BRIEF (ORB)[28]

All these algorithms can be used for the matching of feature points and then for the calculation of the angular changes without manual intervention. Since the focus is on identifying distinguishable points in the scene that can be located after an angular drift, an algorithm that is suitable for corner detection is appropriate for this kind of application. Harris Corner Detection is the standard for the detection of edges and corners, but Shi-Tomasi Corner Detector gives the coordinates of the centroid of the corner to sub-pixel level accuracy. Since this measurement of coordinates of such identified corners is crucial in finding out the angular drift close to the actual drift, the Shi-Tomasi Corner Detector is used to locate the corners or easily distinguished parts of the scene. Figure 4 shows an angular shift of 0° to 5° in both X and Y directions.

After applying Shi-Tomasi Detection of corners in the images of the reference scene and in the image with a rotation of 1° each in both directions, the position of corners in images is captured which gives coordinates of those marked points discussed earlier. Figure 5 gives the position of the marked point (a corner) in the reference scene. All other corners are also shown as red dots in the image.

Similarly, Fig. 6 shows the scene when the camera is affected by an angular drift of 1° in both directions, with red dots as detected corners in the image.

A point in the scene was selected (shown) with an arrow in both the figures above, which was detected in 5 images with different angular shifts. The coordinates of this point in the image were found using the Shi-Tomasi algorithm. Table 3 shows the results obtained by applying the formula given in the previous subsection.

Table 3. Change in image coordinates

	0°	1°	2°	3°	4°
X coordinate	458	574	690	806	922
Y coordinate	408	525	641	757	873

It is observed that the shift in the number of pixels or coordinates of the same point for every degree in either direction is 116, which amounts to a measured shift of 0.9968° for a shift of 1°. Let us calculate the change in angles in the x and y axes using the formulae mentioned previously: -

x_1= 458, x_c= 640 (center of the row in the image as the resolution is (1280 x 960) x_2=574 p = 3.75 x 10^{-6} m (Pixel size is variable for different cameras) f = 25 x 10^{-3} m (Focal length is variable for different optics of the camera)

With these values, angular drift in the X direction is calculated in degrees as in Eqn. 5:

$$\theta_x = \tan^{-1}\frac{3.75\times10^{-6}\times(574-640)}{25\times10^{-3}} - \tan^{-1}\frac{3.75\times10^{-6}\times(458-640)}{25\times10^{-3}} \quad (5)$$

Which gives θ_x = 0.9968° and similarly we will have θ_y = 1.0055°.

Generalizing the above results, the angle of rotation of n° in the x-axis satisfies the following equation for a resolution of $X_c \times Y_c$ having centroid at (x_c, y_c) and a focal length f : -

$$n = \tan^{-1}\frac{n\times0.017455\times\frac{f}{p}+x_0-x_c}{f}\times p - \tan^{-1}\frac{(x_0-x_c)\times p)}{f} \quad (6)$$

It can similarly be generalized for the y-axis, and it has been observed that if x_0 and y_0 are the original position coordinates of the given point, new position coordinates of the point in the image plane for n degree of movement in the camera will be given by the following equations: -

$$x_n = \frac{n\times0.017455\times f}{p} + x_0 \quad (7)$$

$$y_n = \frac{n\times0.017455\times f}{p} + y_0 \quad (8)$$

where,

$\tan 1^o = 0.017455$.

4. OBSERVATIONS & DISCUSSION

Calculations done in the previous subsection have certain assumptions and limitations. It is assumed that the Pixel of the camera sensor is perfectly square i.e., the size given by the value of p does not change ideally. Similarly, it is assumed that the lens of the camera has a focal length along both axes X and Y, and hence, $f_x = f_y = f$. Since all the calculations are dependent on the coordinates of the pixels marked as the centroid of the corner representing a point in space, it is important to maintain a good resolution of the space on the image plane while also maintaining a wide enough image window for the detection of the target.

In the equations Eqn. 1, Eqn. 2, Eqn. 3 & Eqn. 4 for the measurement of the angles of the camera along axes, there are three variables- x or y, p and f and we can discuss the effect of these parameters on the values of θ_x and θ_y.

- x_c and y_c are constant values as per the resolution of the camera
- x and y are coordinates of the detected corner and depend upon three factors: The accuracy of the algorithm to detect the point of interest (a corner in this case), the value of pixel size p, and the focal length f of the camera. These dependencies are explained in the next points.
- p is the pixel size or the side of the smallest sensing unit in a camera that captures a certain size of a square block of space in the real world. If f is kept constant and p is reduced, it can resolve the space better and hence will give a more accurate measurement of the coordinates of the centroid of the corners. But decreasing the value of p choosing a camera sensor with a smaller pixel size will reduce the image window size at a constant distance from the camera. To maintain the image window size, the resolution of the sensor has to be increased, which further increases the time of execution of algorithms as a drawback, which mostly consists of operations on pixels or groups of pixels.
- f is the focal length of the optics and it controls the image window or Field-Of-View (FOV) of the camera system. If p is kept fixed, increasing the value of f will decrease the FOV and hence the space is resolved better in pixels with more details, and hence will increase the accuracy of

measurement of the coordinates of corners as discussed in the previous paragraph also.

These trade-offs between FOV and Accuracy are shown in Table 4 representing the effect of these changes on crucial specifications:

Table 4. Trade-off between important parameters

Pixel size (p)	Focal length (f)	FOV	Accuracy
Increase	Constant	Increase	Decrease
Decrease	Constant	Decrease	Increase
Constant	Increase	Decrease	Increase
Constant	Decrease	Increase	Decrease

5. CONCLUSION

If we try to tune the system for different values of p and f, there is a trade-off between FOV and the Accuracy of the measurement by the algorithm. Since through the current exercise, we are trying to compensate for the angular drift to the camera in both axes before the measurement of the trajectory of the shell, accuracy is a lot more crucial than the FOV and hence we can increase the focal length and decrease the pixel size to achieve higher accuracy in measurement of values of angular drift.

5.1 Offset Compensation Method against Ground Shake

We can now devise a compensation method for the effects caused by the shaking of the ground. Figure 7, which is self-explanatory and covers whatever was discussed in previous subsections, gives the scheme for the process followed. This process is for the effect of a shake before the measurement of the trajectory of the shell, which must be tracked in real-time as the end goal of this problem. The effect of Ground shake on the measurement of the trajectory of the shell while in operation, whenever there is a shake of the camera during measurement, is explained in the next section.

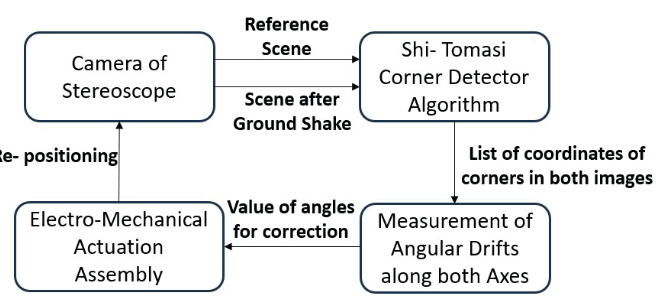

Figure 7. Offset compensation against ground shake.

REFERENCES

1. Habib, A.; Detchev, I. & Kwak, E. Stability analysis for a multi-camera photogrammetric system. *Sensors*, 2014, **14**(8), 15084–15112. doi: 10.3390/s140815084.
2. Liu, J.; Zhao, J.; Lin, L.; Zhang, Y. & Liu, Y. Analysis of the development direction of small-medium caliber artillery. *J. Phys. Conf. Ser.*, 2023, **2460**(1), 012069. doi: 10.1088/1742-6596/2460/1/012069.
3. Sharma, M. & Kar, S. Estimation of trajectory of high-speed artillery shell. *Def. Sci. J.*, 2023, **73**(3). doi: 10.14429/dsj.73.18342.
4. Wang, I.-T. Field experiments and numerical analysis of the ground vibration isolation of shock wave propagation under explosion shock loading. *Vibration*, 2019, **2**(4). doi: 10.3390/vibration2040019.
5. Singh, P.K. & Roy, M.P. Damage to surface structures due to blast vibration. *Int. J. Rock Mech. Min. Sci.*, 2010, **47**(6), 949–961. doi: 10.1016/j.ijrmms.2010.06.010.
6. Werner, S.D. Engineering characteristics of earthquake ground motions. *Nucl. Eng. Des.*, 1976, **36**(3), 367–395. doi: 10.1016/0029-5493(76)90029-7.
7. Goda, K.; Pomonis, A.; Chian, Siau Chen; Offord, Mark; Saito, Keiko; Sammonds, Peter; Fraser, Stuart; Raby, Alison & Macabuag, J. Ground motion characteristics and shaking damage of the 11th March 2011 Mw9.0 Great East Japan earthquake. *Bull. Earthq. Eng.*, 2013, **11**(1), 141–170. doi: 10.1007/s10518-012-9371-x.
8. Lee, Y.-T.; Ma, K.-F.; Wang, Y.-J. & Wen, K.-L. An empirical equation of effective shaking duration for moderate to large earthquakes. *Nat. Hazards*, 2015, **75**(2), 1779–1793. doi: 10.1007/s11069-014-1398-7.
9. Hartley, R. & Sturm, P. Triangulation, *Comput. Vis. Image Underst.*, 2001, **68**(146–157). doi: 10.1006/cviu.1997.0547.
10. Liu, Y.; Ge, Z.; Yuan, Y.; Su, X.; Guo, X.; Suo, T. & Yu Q. Study of the error caused by camera movement for the stereo-vision system. *Appl. Sci.,* 2021, **11**, 9384. doi: 10.3390/app11209384.
11. Shao, X. & He, X. Camera motion-induced systematic errors in stereo-DIC and speckle-based compensation method. *Opt. Lasers Eng.*, 2022, **149**, 106809. doi: 10.1016/j.optlaseng.2021.106809.
12. Meng, Z.; Kong, X.; Meng, L. & Tomiyama, H. Camera motion estimation and optimization approach. *In* 2019 International Conference on Advanced Mechatronic Systems (ICAMechS), 2019, pp. 212–217. doi: 10.1109/ICAMechS.2019.8861680.
13. Hirschmuller, H.; Innocent, P.R. & Garibaldi, J.M. Fast, unconstrained camera motion estimation from stereo without tracking and robust statistics. *In* 7th International Conference on Control, Automation, Robotics and Vision, 2002. ICARCV 2002., 2002, **2**, pp. 1099–1104. doi: 10.1109/ICARCV.2002.1238577.
14. e Souza, M.R.; de Almeida Maia, H. & Pedrini, H. Rethinking two-dimensional camera motion estimation assessment for digital video stabilization: A camera motion field-based metric. *Neurocomputing*, 2023, **559**, 126768. doi: 10.1016/j.neucom.2023.126768.
15. Zhang, Y.; Zhang, W.; Zhao, X. & Yuan, H. Study on electronic image stabilization system based on MEMS gyro. *In* 2009 International Conference on Electronic Computer Technology, 2009, pp. 641–643. doi: 10.1109/ICECT.2009.27.

16. Wenshuang, Wu; Huajun, F.; Lirong, H.; Zhihai, X.; Qi, L.; Yueting, C.; Chenwei, Y. & Zhenzhen, Z. A method for remote sensing image restoration using gyroscope sensor. 2017, p. 79.
doi: 10.1117/12.2283540.
17. Li, S.; Gao, Y.; Meng, G.; Wang, G. & Guan, L. Accelerometer-based gyroscope drift compensation approach in a dual-axial stabilization platform. *Electronics*, 2019, **8**(5).
doi: 10.3390/electronics8050594.
18. Koh, I.-S.; Ro, S.-Y.; Kim, J.-P.; Min, K. yuk & Chong, J. A novel digital image stabilization for mobile applications. 2011.
doi: 10.1109/ICCE.2011.5722544.
19. Wang, K. Experiment research on electronic image stabilization of omni-directional camera system. *In* 2011 IEEE 18th International Conference on Industrial Engineering and Engineering Management, 2011, pp. 1682–1685.
doi: 10.1109/ICIEEM.2011.6035485.
20. Deng, Z.; Yang, D.; Zhang, X.; Dong, Y.; Liu, C. & Shen, Q. Real-time image stabilization method based on optical flow and binary point feature matching. *Electronics*, 2020, **9**(1).
doi: 10.3390/electronics9010198.
21. Pizarro, A.; Dal Sasso, S.F. & Manfreda, S. VISION: VIdeo StabilisatION using automatic features selection for image velocimetry analysis in rivers. *SoftwareX*, 2022, **19**, 101173.
doi: 10.1016/j.softx.2022.101173.
22. Harris, C.; & Stephens, M. A combined corner and edge detector. Proceedings of the Alvey Vision Conference 1988, Manchester: Alvey Vision Club, 1988, **6**, p. 23.1-23.
doi: 10.5244/C.2.23.
23. Shi, J. & Tomasi. Good features to track. 1994 Proceedings of IEEE Conference on Computer Vision and Pattern Recognition, 1994, pp. 593–600.
doi: 10.1109/CVPR.1994.323794.
24. Lindeberg, T. scale invariant feature transform. *Scholarpedia*, 2012, **7**.
doi: 10.4249/scholarpedia.10491.
25. Bay, H.; Tuytelaars, T. & Van Gool, L. SURF: Speeded up robust features. In computer vision – ECCV 2006, A. Leonardis, H. Bischof, and A. Pinz, Eds., Berlin, Heidelberg: Springer, 2006, pp. 404–417.
doi: 10.1007/11744023_32.
26. Rosten, E. & Drummond, T. Machine learning for high-speed corner detection. In computer vision – ECCV 2006, A. Leonardis, H. Bischof, and A. Pinz, Eds., Berlin, Heidelberg: Springer, 2006, pp. 430–443.
doi: 10.1007/11744023_34.
27. Calonder, M.; Lepetit, V.; Strecha, C. & Fua, P. BRIEF: Binary robust independent elementary features. *In* European Conference on Computer Vision. Sep. 2010, pp. 778–792.
doi: 10.1007/978-3-642-15561-1_56.
28. Rublee, E.; Rabaud, V.; Konolige, K. & Bradski, G. ORB: An efficient alternative to SIFT or SURF. *In* 2011 International Conference on Computer Vision, Nov. 2011, pp. 2564–2571.
doi: 10.1109/ICCV.2011.6126544.

CONTRIBUTORS

Mr Manoj Sharma is working as a Scientist at DRDO. His areas of interest include: Optoelectronic sensors and systems for defense applications.
His contribution to the proposed work include: Simulations, the generation of videos, and verifying the idea through results applying image processing algorithms and also register, analyse and document the results to prepare the proposed paper.

Mr Subrat Kar is working as a Professor in the Department of Electrical Engineering at IIT Delhi. His research interests include: Optics, embedded telecom systems, transmission and switching, automotive networks, deep space communications, and biomedical instrumentation.
His contribution to the proposed paper include: Original idea of a multiple-camera-based system to replace bulkier and costly radar-based counter-battery systems in artillery combat and brainstorming on the limiting factors of the proposed system. He guided the main author all through the implementation of the idea.

Mr Sumantra Dutta Roy is working as a Professor in the Department of Electrical Engineering at IIT Delhi. His research interest include: Computer vision and image analysis, pattern recognition and machine learning, medical informatics, biometrics, bioinformatics, and music information retrieval and analysis.
His contribution in the proposed paper is to guide main author on image processing algorithms that are suitable to implement the method proposed to measure the shake in the camera.